

Color Discrimination in Color Vision Deficiency: Photon-Assisted Piezoelectric IGZO Color-Tactile Sensors with P(VDF-TrFE)/Metal-Decorated TiO₂-Nanofibers Nanocomposites

Yi-Pei Jiang, Ming-Chung Wu, Ting-Han Lin, Yin-Hsuan Chang, and Jer-Chyi Wang*

According to the Colour Blind Awareness organization's report, color vision deficiency, including color blindness and partial tritanopia, affects ≈300 million people worldwide. However, those affected can only improve their color vision deficiency by color light training and stimulation therapies or through contact lenses to correct vision with limited effectiveness. Herein, the photon-assisted piezoelectric indium–gallium–zinc oxide (IGZO) color-tactile sensors coated with poly(vinylidene fluoride-co-trifluoroethylene) (P(VDF-TrFE)) copolymers blended with metal-decorated TiO₂-nanofibers (NFs) have been investigated to boost the piezoelectric response at tunable wavelengths of light. Prior to the device fabrication, material analysis is performed to confirm the blending of metal-decorated TiO₂-NFs in P(VDF-TrFE) copolymers and the absorption of the three primary colors of light. By optimizing the blending percentage, the ferroelectric behaviors of the nanocomposites are significantly improved owing to the enhanced crystallinity of the β-phase. With the illumination of red, green, and blue lights, the photons are effectively absorbed by Ag-, Au-, and Y-decorated TiO₂-NFs, respectively. These absorptions generate electron–hole pairs via localized surface plasmon resonance for the enhanced piezoelectric response of IGZO color-tactile sensors, allowing people with deficient color vision to perceive different light colors by a touch motion.

1. Introduction

The human eye is the only organ that acquires external visual information and transmits signals to the brain. It has been reported that more than 80% of the knowledge and memory within a brain is received by the eyes.^[1–3] Two retinal photoreceptor cells in the human eyes, rod and cone cells, are responsible for scotopic/peripheral and photopic/color vision, respectively.^[4,5] Additionally, cone cells identify three primary colors: red, green, and blue. When genetic or acquired factors affect the function of cone cells, abnormal color discrimination is observed. People who cannot use visual learning are visually impaired, accounting for 8% of the global population.^[6–8] These include total blindness with the loss of light perception, amblyopia with low vision, and color vision deficiencies such as color blindness and partial tritanopia. To consider the needs of people with deficient color vision, distinguishing between colors is one of the capabilities that can make their daily

Y.-P. Jiang, J.-C. Wang
Department of Electronic Engineering
Chang Gung University
Guishan Dist., Taoyuan 33302, Taiwan
E-mail: jcwang@mail.cgu.edu.tw

M.-C. Wu, T.-H. Lin, Y.-H. Chang
Department of Chemical and Materials Engineering
Chang Gung University
Guishan Dist., Taoyuan 33302, Taiwan

M.-C. Wu, J.-C. Wang
Green Technology Research Center
Chang Gung University
Guishan Dist., Taoyuan 33302, Taiwan

M.-C. Wu
Division of Neonatology
Department of Pediatrics
Chang Gung Memorial Hospital, Linkou
Guishan Dist., Taoyuan 33305, Taiwan

J.-C. Wang
Department of Neurosurgery
Chang Gung Memorial Hospital, Linkou
Guishan Dist., Taoyuan 33305, Taiwan

J.-C. Wang
Department of Electronic Engineering
Ming Chi University of Technology
Taishan Dist., New Taipei City 243303, Taiwan

 The ORCID identification number(s) for the author(s) of this article can be found under <https://doi.org/10.1002/admt.202101147>.

DOI: 10.1002/admt.202101147

life more convenient. At present, the only improvement opportunities for color vision deficient people are color light training, stimulation therapies, and through contact lens correction;^[9–11] however, their effects are limited with relatively high costs. Hence, it is vital for people with deficient color vision to gain photosensitivity quickly and effectively to integrate into society.

Recently, emerging piezoelectric polymer materials have shown great potential for transferring mechanical forces into electrical signals. To meet the requirements of biomedicines, energy harvesters, and self-powered systems, materials with hybrid properties including piezoelectricity, phototronic effects, photovoltaics, and photoexcitation have attracted everyone's attention.^[12–14] In 2010, Wang et al. proposed a piezoelectric material coupled with a phototronic effect for a new application in bimodal piezo-phototronic devices. The basic principle of piezo-phototronicity is that the piezoelectric potential generated by the strain is applied to control the generation, transmission, separation, and recombination of carriers at the metal-semiconductor heterojunction or PN junction, thereby improving the characteristics of optoelectronic devices.^[15–18] It has been implemented in photodetectors with CH₃NH₃PbI₃ perovskite thin films, solar cells with carbon-fiber/ZnO-CdS double-shell microwires, and light-emitting diodes with the composite materials of photoactive Ag₂O and piezoelectric BaTiO₃.^[19–22] It is worth noticing that the piezo-phototronicity of these devices can be observed distinctly under the strain or optical environments, which is also called the piezo-enhanced phototronic effect. In contrast to piezo-phototronicity, in this study, a new photon-assisted piezoelectric effect is proposed to identify different colors of light under the application of a strain. It is crucial to develop photon-assisted piezoelectricity to benefit specific groups of people, especially those with deficient color vision.

Poly(vinylidene fluoride-co-trifluoroethylene) (P(VDF-TrFE)) is a fascinating piezoelectric copolymer that exists in four different phases: α , β , γ , and δ . Among these phases, the β -phase is the main feature to achieve high piezoelectricity of P(VDF-TrFE).^[23–25] Additionally, introducing semiconducting fillers, such as TiO₂ and Mo, can further enhance the β -phase in P(VDF-TrFE) using a solution casting technique.^[26,27] TiO₂, a wide indirect bandgap semiconductor that enables the absorption of only UV light, is beneficial to the mechanical properties of P(VDF-TrFE) copolymers. 1D TiO₂ nanostructures such as TiO₂ nanofillers (TiO₂-NFs) show an enlargement of the surface area, a reduced ion transport length, and an efficient transport of carriers along the 1D trajectory, which is favorable for piezoelectric applications.^[28–31] The decoration of TiO₂ with metals can further achieve a tunable optical absorption behavior. A series of comprehensive metal-decorated TiO₂ has yielded significant implications for applications in piezoelectric devices.^[32–35] For the metal-loaded TiO₂-NFs, metal deposition induces photon absorption into visible light and facilitates electron migration to TiO₂-NFs,^[36–38] which results from localized surface plasmon resonance (LSPR). In this study, we report a series of P(VDF-TrFE)/TiO₂-NFs nanocomposites with the deposition of silver (Ag), gold (Au), and yttrium (Y) on a TiO₂-NF surface to achieve an enhanced piezoelectric response at tunable wavelengths of light. With the optimized concentration of 5 ppm of the metal-decorated TiO₂-NFs blended in P(VDF-TrFE) copolymers, the

ferroelectric properties of the metal-ferroelectric-metal (MFM) capacitors were significantly improved owing to the enhanced crystallinity of the β -phase for further applications in piezoelectricity. The Ag-, Au-, and Y-decorated TiO₂-NFs blended in P(VDF-TrFE) copolymers were discovered to respond notably well to the colors of red, green, and blue light, respectively, through the monitoring of the change in drain current of the indium-gallium-zinc oxide (IGZO) color-tactile sensors under the application of an external force. The built-in electric field of the dipole moments within the P(VDF-TrFE)/metal-decorated TiO₂-NFs nanocomposite films separated the photogenerated electron-hole pairs to demonstrate photon-assisted piezoelectricity. The superior bimodal effect can be implemented in future organic pressure sensors and aims to benefit people with deficient color vision to identify different colors of light on a light-emitting diode (LED) panel with the alphabet and on a tablet with a pseudoisochromatic plate by a simple touch motion.

2. Results and Discussion

2.1. Material Analyses of Metal-Decorated TiO₂-NFs Blended in P(VDF-TrFE) Copolymers

To enhance the crystallinity of the P(VDF-TrFE) films blended with metal-decorated TiO₂-NFs for better electrical properties, the photo-thermal annealing instead of the conventional thermal annealing was performed in this study, as shown in Figure S1, Supporting Information. **Figure 1a–c** shows the X-ray diffraction (XRD) patterns of the P(VDF-TrFE)/metal-decorated TiO₂-NFs nanocomposite films, which leads to the change in β -phase. In the XRD patterns, the characteristic peak was observed at 19.96° corresponding to (200) of the β -phase.^[39] After introducing the Ag-, Au-, and Y-decorated TiO₂-NFs, all XRD patterns showed an increment in peak intensity with an increase in nanofiller concentration. Additionally, the shift of diffraction peaks towards a lower diffraction angle demonstrated the increment in lattice spacing or lattice expansion.^[40] The Fourier-transform infrared (FTIR) spectroscopy provides further information on the induced phase formation of the P(VDF-TrFE)/metal-decorated TiO₂-NFs nanocomposites, as presented in Figure 1d–f. The peaks at 840, 1285, and 1400 cm⁻¹ confirm the existence of a polar β -phase for P(VDF-TrFE) copolymers.^[41,42] The –C–F symmetric stretch was assigned to 840 cm⁻¹. The CCC scissoring vibration, C–C symmetric stretching, and CF₂ asymmetric stretching in the β -phase of P(VDF-TrFE) were indicated at 1285 cm⁻¹. Furthermore, the peak at 1400 cm⁻¹ characterizes the –C–C– asymmetric stretching and the wagging frequency of the –CH₂ bond. Evidently, with increasing amounts of TiO₂-NFs in P(VDF-TrFE) copolymers, the enhancement of the polar β -phase became more significant. Morphological investigations of the P(VDF-TrFE)/metal-decorated TiO₂-NFs nanocomposite films were examined by field-emission scanning electron microscopy (FE-SEM) (see Figure 1g–p). In general, the P(VDF-TrFE) film presents homogeneous needle-like crystals embedded in the matrix of PVDF.^[43] With the blending of TiO₂-NFs, the increased crystallinity could result in the formation of more needle-like crystals. Additionally, in Figure 1q, the energy-dispersive

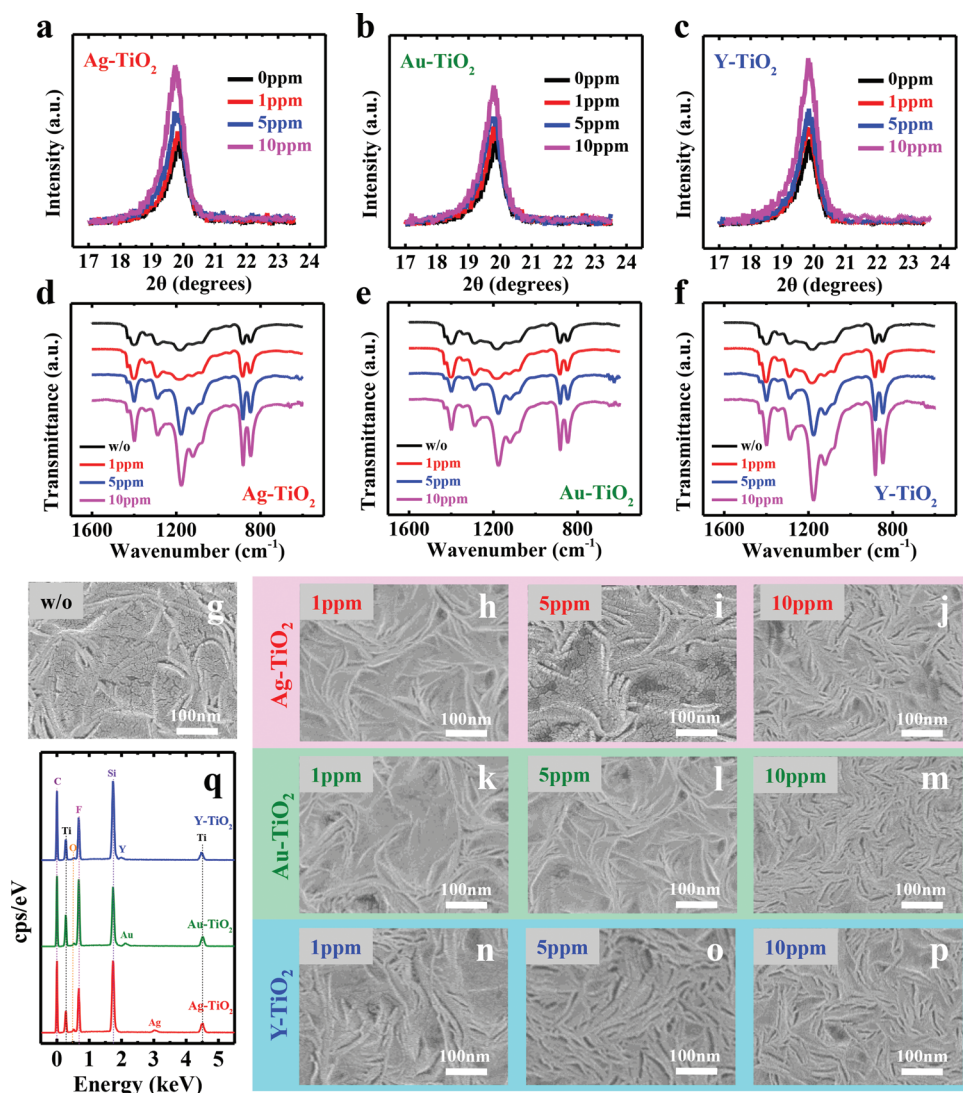


Figure 1. XRD patterns and FTIR spectra of the P(VDF-TrFE) copolymers blended with a,d) Ag-, b,e) Au-, and c,f) Y-decorated TiO₂-NFs, respectively, with the blending percentages of 1 to 10 ppm; FE-SEM morphological images of g) the pure P(VDF-TrFE) film and the films blended with h–j) Ag-, k–m) Au-, and n–p) Y-decorated TiO₂-NFs with the blending percentages of 1, 5, and 10 ppm, respectively; q) EDS spectra of the P(VDF-TrFE) copolymers blended with Ag-, Au-, and Y- decorated TiO₂-NFs, confirming the successful decoration of metal-NPs on the TiO₂-NFs.

X-ray spectroscopy (EDS) spectra show the presence of Ag, Au, and Y elements, which confirm that the metal-NPs were successfully decorated on the TiO₂-NFs. To further investigate the comprehensive microstructures of Ag-, Au-, and Y-decorated TiO₂-NFs, the high-resolution transmission electron microscopy (HRTEM) images were acquired and are shown in Figure S2a–f, Supporting Information. It was observed that the as-synthesized TiO₂-NFs showed a typical fiber-like structure with a uniform surface. Moreover, diameters of the TiO₂-NFs ranging from 50 to 110 nm were obtained. The metal-NPs randomly precipitated on the surface of the TiO₂-NFs with an average diameter of 6.23, 9.03, and 1.90 nm for Ag-, Au-, and Y-NPs, respectively, as shown in the statistical distributions of Figure S2g–i, Supporting Information.

The ultraviolet–visible (UV–Vis) diffuse reflectance spectra of Ag-, Au-, and Y-decorated TiO₂-NFs were investigated and are

shown in Figure 2a. Ag-decorated TiO₂-NFs showed broad and intense visible region absorption from 522 to 750 nm. Moreover, Au-decorated TiO₂-NFs exhibited enhanced visible-light absorption with a maximum wavelength of 521 nm. A remarkable enhancement was observed at 450 nm for the Y-decorated TiO₂-NFs. We can postulate that the significant enhancement of the absorption in the specific region of visible light for each material is attributed to the LSPR of metal-NPs decorated on TiO₂-NFs. The free electrons localized on the metal-NPs showed strong interaction with the incident electromagnetic waves and further strengthened the absorption of visible light. To clarify the electron extraction capability, lights of various wavelengths, including 650, 530, and 450 nm, were switched on during scanning. We conducted the surface potential mapping of pure P(VDF-TrFE) and Ag-, Au-, and Y-decorated TiO₂-NFs blended P(VDF-TrFE) copolymers, as presented in Figure 2b–m. The

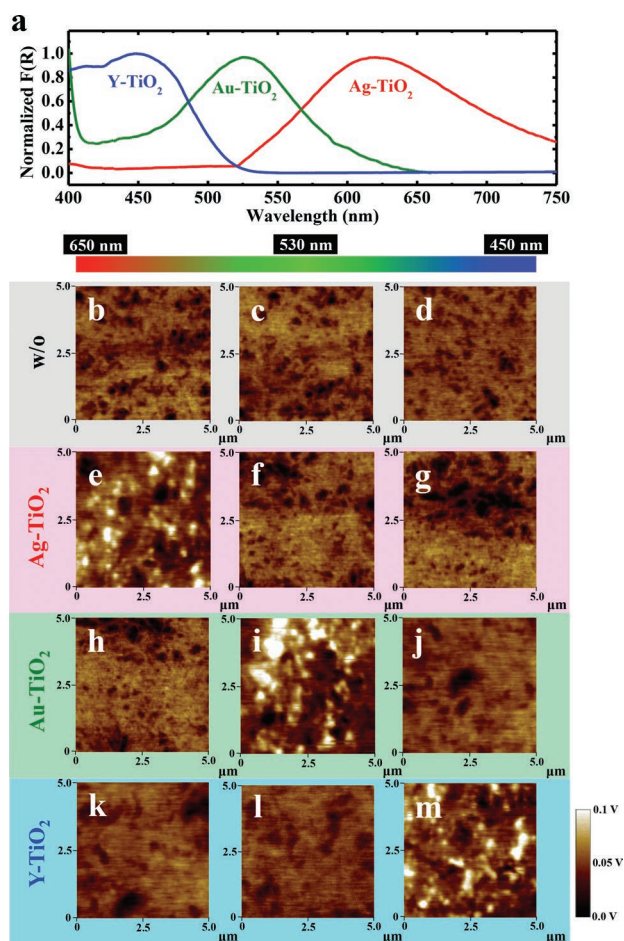


Figure 2. a) UV-Vis diffuse reflectance spectra of Ag-, Au-, and Y-decorated TiO_2 -NFs, showing the absorption in the specific region of visible light for each material; KPFM surface potential mapping of b–d) the pure P(VDF-TrFE) film and the films blended with e–g) Ag-, h–j) Au-, and k–m) Y-decorated TiO_2 -NFs under the light irradiation of 650, 530, and 450 nm, respectively.

potential mapping of the P(VDF-TrFE) film obtained by Kelvin probe force microscopy (KPFM) presented a similar contact potential difference under various wavelengths of light. After introducing Ag-, Au-, and Y-decorated TiO_2 -NFs into P(VDF-TrFE), the surface potential increased significantly under light irradiation at 650, 530, and 450 nm, respectively. This result elucidates that the metal-decorated TiO_2 -NFs facilitated the photon-induced electron migration to TiO_2 -NFs, which could be advantageous for further piezoelectric applications.

2.2. Ferroelectric, Piezoelectric, and Phototronic Behaviors of P(VDF-TrFE) Copolymers Blended with Metal-Decorated TiO_2 -NFs

The polarization versus electric field (P - E) characteristics of the MFM capacitors with the P(VDF-TrFE) films blended with Ag-, Au-, and Y-decorated TiO_2 -NFs were measured and are shown in Figure S3a–c, Supporting Information, respectively. The rem-

nant polarization ($2P_r$) of the MFM capacitors with pure P(VDF-TrFE) appeared to be $5.3 \mu\text{C cm}^{-2}$. In contrast, for the devices with the P(VDF-TrFE) films blended with Ag-, Au-, and Y-decorated TiO_2 -NFs of 1 to 10 ppm, the $2P_r$ increased significantly to at least 6.56, 6.01, and $6.91 \mu\text{C cm}^{-2}$, respectively. The $2P_r$ can be optimized for nanocomposite films with 5-ppm metal-decorated TiO_2 -NFs. Additionally, the coercive electric field (E_c) decreased from 0.392 MV cm^{-1} for the MFM capacitors with pure P(VDF-TrFE) films to 0.302, 0.316, and 0.235 MV cm^{-1} for those with 5-ppm Ag-, Au-, and Y-decorated TiO_2 -NFs blended films, respectively. The increased $2P_r$ and decreased E_c values imply that the photo-thermal annealing process on the P(VDF-TrFE) films blended with metal-decorated TiO_2 -NFs can enhance the ferroelectric characteristics, which is ascribed to the enhanced crystallinity of the P(VDF-TrFE) copolymers. To further confirm the effectiveness of the photo-thermal annealing, the ferroelectric properties of the P(VDF-TrFE) films blended with 5-ppm metal-decorated TiO_2 -NFs before and after the annealing process were investigated, as shown in Figure S4, Supporting Information. However, as presented in the XRD, FTIR, and FE-SEM results shown in Figure 1, the crystalline domains were strengthened with an increase in the concentration of metal-decorated TiO_2 -NFs. To determine the reasons for the degraded ferroelectric characteristics in the P(VDF-TrFE) films blended with 10-ppm metal-decorated TiO_2 -NFs, the DC current versus electric field (I - E) characteristics were measured and are shown in Figure S3d–f, Supporting Information. The leakage current of the pure P(VDF-TrFE) films was $\approx 1.19 \times 10^{-11} \text{ A}$ under an electric field of 0.4 MV cm^{-1} . It can be seen that the leakage current increased gradually with an increased concentration of metal-decorated TiO_2 -NFs in P(VDF-TrFE) films at both the positive and negative biases, worsening the ferroelectricity of the nanocomposite films. Considering the crystallinity and leakage current simultaneously, the P(VDF-TrFE) films blended with 5-ppm metal-decorated TiO_2 -NFs exhibited the optimal ferroelectric behaviors.

To realize the functionality of color discrimination, the IGZO color-tactile sensors coated with the P(VDF-TrFE) copolymers blended with metal-decorated TiO_2 -NFs were fabricated, as illustrated in Figure S5, Supporting Information. Figures S6 and S7, Supporting Information, show the typical drain current versus back-gate bias ($I_{\text{DS}}-V_{\text{BG}}$) transfer characteristics of the sensors measured at $V_{\text{DS}} = 0.1 \text{ V}$ with V_{BG} swept from -5 to 25 V . A stimulated force of 0 to 400 g was applied, and the external white light of 0 to 1500 lx was illuminated on the devices. From these figures, it can be concluded that only the piezoelectric but no phototronic responses of the IGZO color-tactile sensors were observed, which is different from the previously proposed piezo-phototronic devices.^[44,45] Conversely, if the stimulated force was applied, the drain current of the devices coated with the P(VDF-TrFE)/metal-decorated TiO_2 -NFs nanocomposite films gradually increased with an increase in the illuminance of external light, as shown in Figure S8, Supporting Information, implying that the piezoelectric effect can be enhanced by phototronicity. To further investigate the enhancement in the drain current of the devices coated with the nanocomposite films with different concentrations of metal-decorated TiO_2 -NFs and different illuminances of the three primary colors of light, the current response was calculated according to Equation (1) and

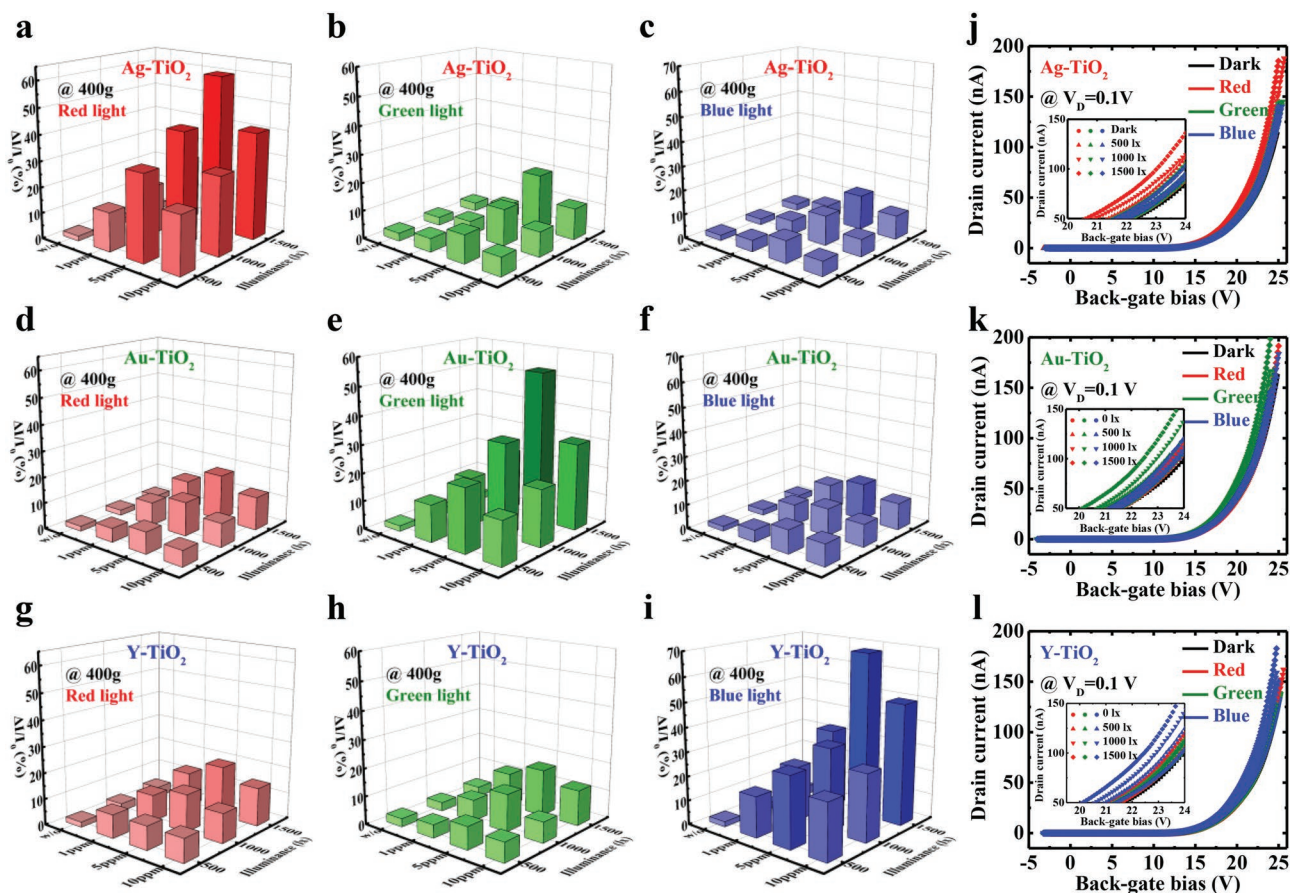


Figure 3. 3D contours in the current response of the IGZO color-tactile sensors coated with the P(VDF-TrFE) copolymers blended with different concentrations of a–c) Ag-, d–f) Au-, and g–i) Y-decorated TiO₂-NFs under different illuminances of red, green, and blue colors of light, respectively, at the stimulated force of 400 g; the I_{DS} – V_{BG} transfer characteristics of the IGZO color-tactile sensors coated with the P(VDF-TrFE) films with j) Ag-, k) Au-, and l) Y-decorated TiO₂-NFs of 5 ppm under different illuminances and colors of light at the stimulated force of 400 g with the magnified scale of the curves shown in the inset figures.

is plotted in the 3D contours of **Figure 3a–i** and Figures S9–S11, Supporting Information:^[46]

$$\text{Current response} = \left(\frac{I - I_0}{I_0} \right) \times 100\% = \left(\frac{\Delta I}{I_0} \right) \times 100\% \quad (1)$$

where I and I_0 are the drain currents with and without the illumination of external light under different stimulated forces, respectively. For the IGZO color-tactile sensors coated with the P(VDF-TrFE) copolymers blended with metal-decorated TiO₂-NFs, the highest current response under an illuminance of 1500 lx can be observed for the three primary colors of light. Additionally, the current response of the devices coated with the P(VDF-TrFE) films blended with Ag-, Au-, and Y-decorated TiO₂-NFs was more sensitive to the red, green, and blue colors of light, respectively, which is consistent with the response of the absorption spectra in Figure 2. The concentration of metal-decorated TiO₂-NFs in P(VDF-TrFE) films for the current response of IGZO color-tactile sensors under different illuminances and colors of light was optimized at 5 ppm, where the I_{DS} – V_{BG} transfer characteristics under the stimulated force of 400 g are illustrated in Figure 3j–l. The curves plotted on a

magnified scale are shown in the inset figures to clearly identify the change in drain current under different illuminances of the three primary colors of light. In contrast, the I_{DS} – V_{BG} transfer characteristics of the IGZO color-tactile sensors coated with the pure P(VDF-TrFE) films under different illuminances and colors of light were also investigated, as shown in Figure S12, Supporting Information. The curves are almost identical, meaning that there is no color discrimination ability for the devices coated with the pure P(VDF-TrFE) copolymers.

2.3. Photon-Assisted Piezoelectric Behaviors of IGZO Color-Tactile Sensors Coated with P(VDF-TrFE) Copolymers Blended with Metal-Decorated TiO₂-NFs

The current increment versus time (ΔI – t) characteristics of the IGZO color-tactile sensors coated with the P(VDF-TrFE) copolymers blended with metal-decorated TiO₂-NFs were measured under different stimulated forces and illuminances of the three primary colors of light, as shown in **Figure 4a–f**. The current increment was recorded by first applying the force before illuminating the light and then in reverse order to verify the

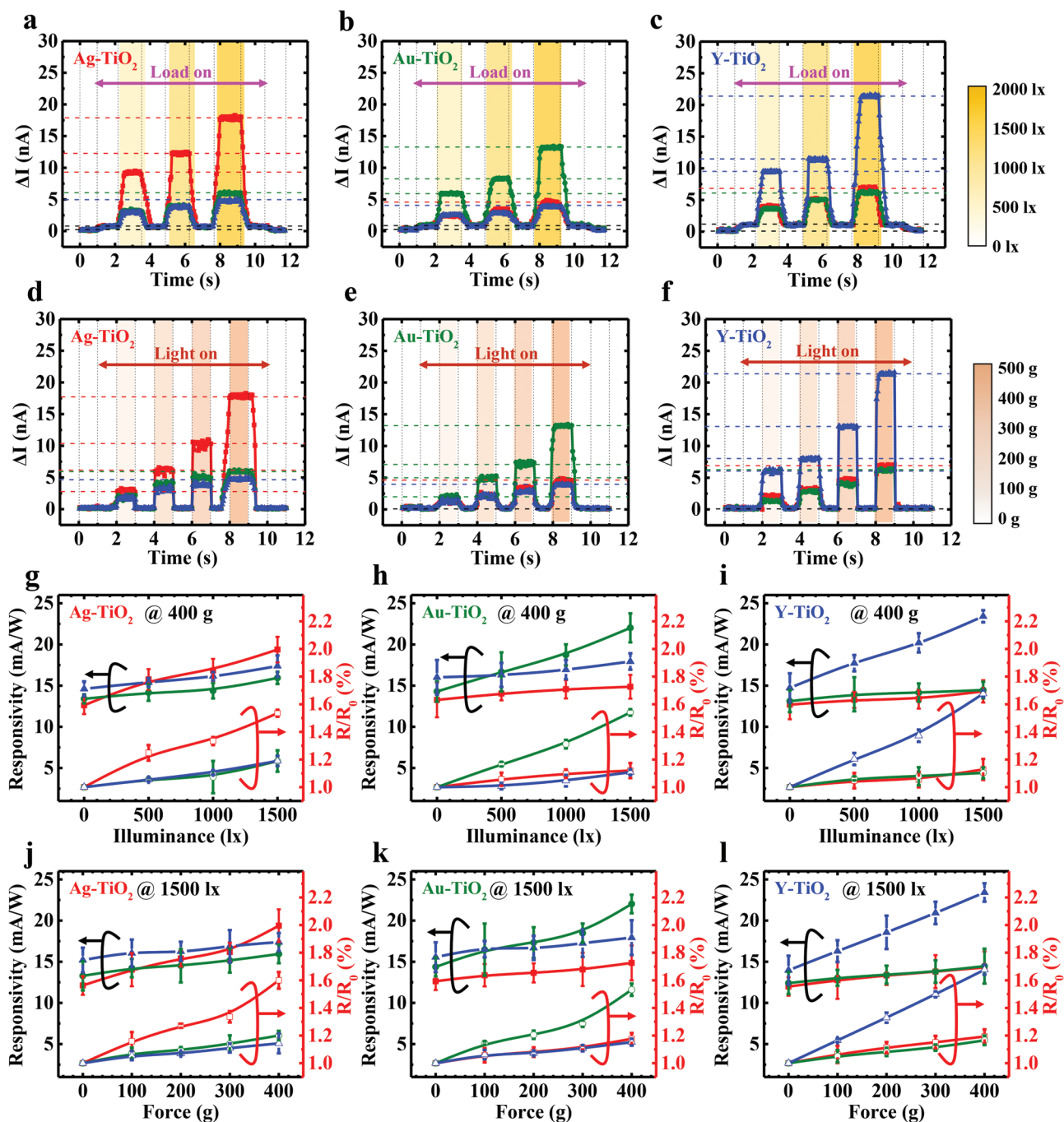


Figure 4. ΔI - t characteristics of the IGZO color-tactile sensors coated with the P(VDF-TrFE) copolymers blended with a,d) Ag-, b,e) Au, and c,f) Y-decorated TiO_2 -NFs under different stimulated forces and illuminances of three primary colors of light. In a–c), the response can be divided into two blocks: one is the block for the sensors under a stimulated force of 400 g and denoted as load-on; the other is the block for the sensors under different illuminances of light and painted in orange color. Additionally, in d–f), the response can also be divided into two blocks: one is the block for the sensors under a light illumination of 1500 lx and denoted as light-on; the other is the block for the sensors under the stimulated forces of 100 to 400 g and painted in brown color. The responsivity and enhancement factor of the IGZO color-tactile sensors coated with the P(VDF-TrFE) copolymers blended with g,j) Ag-, h,k) Au, and i,l) Y-decorated TiO_2 -NFs under different illuminances of light at a stimulated force of 400 g and under various stimulated forces at a light illumination of 1500 lx, respectively. The filled and open symbols with red squares, green circles, and blue triangles show average responsivity and enhancement factor, respectively, obtained from 10 different sensors with the error bars representing S.D.

photon-assisted piezoelectric effect, as presented in Figure 4a–c and 4d–f, respectively. In Figure 4a–c, the response can be divided into two blocks: one is the block for the sensors under

a stimulated force of 400 g and denoted as load-on; the other is the block for the sensors under different illuminances of light and painted in an orange color. In the first stage, the current

increment was ≈ 1.65 nA for the sensors under a stimulated force. Subsequently, an external light of 500, 1000, and 1500 lx was illuminated, and the current was significantly increased depending on the red, green, and blue colors of light. The illumination of a specific color of light can bring about the photon-assisted piezoelectric effect on the IGZO color-tactile sensors, manifesting the capability of color discrimination due to the difference in color absorption capacity among Ag-, Au-, and Y-decorated TiO₂-NFs in P(VDF-TrFE) films. Notably, the current increment returned to ≈ 1.65 nA whenever the external light source was removed. The current increment contributed only by the piezoelectric effect via a stimulated force. On the other hand, in Figure 4d–f, the response can also be divided into two blocks: one is the block for the sensors under a light illumination of 1500 lx and denoted as light-on; the other is the block for the sensors under the stimulated forces of 100 to 400 g and painted in a brown color. Initially, when the external light was illuminated without any stimulated force, there was no increase in the current. Once the force was applied, the current increment was clearly observed and increased to the same level as the sensors under both the stimulated force of 400 g and the external light of 1500 lx in Figure 4a–c. Nonetheless, whenever the force was removed, the current increment was reduced to zero. Considering the sequence of the application of force and the illumination of light, we can conclude that the light illumination can only enhance the piezoelectric effect of the IGZO color-tactile sensors. To further analyze the color discrimination capability of these sensors, the responsivity was calculated according to the following equation:^[47]

$$R = \frac{\Delta I}{P_1} \quad (2)$$

where R is the responsivity of the photon-assisted piezoelectric effect, ΔI is the current enhanced by the external light under a stimulated force, and P_1 is the power of light illumination in watts. As shown in Figure 4g–i, the responsivity of the IGZO color-tactile sensors increased with the increase in illuminance, particularly for the matching of the color of light with metal-decorated TiO₂-NFs. Additionally, when the stimulated force increased (Figure 4j–l), the responsivity of the photon-assisted piezoelectric effect was enhanced significantly, implying that the piezoelectric dipole moment in P(VDF-TrFE) copolymers can help the photon-induced electrons to be injected into the IGZO channel and further increase the drain current. Meanwhile, the relative change in responsivity, also defined as the enhancement factor, was calculated using the following equation:^[48]

$$\text{Enhancement factor} = \frac{R}{R_0} \times 100\% \quad (3)$$

where R_0 is the responsivity without illumination. With the increase in illuminance from 0 to 1500 lx (Figure 4g–i) and stimulated force from 100 to 400 g (Figure 4j–l), the enhancement factor of the IGZO color-tactile sensors increased, particularly for the matching of the color of light with metal-decorated TiO₂-NFs; that is, the R/R_0 of the sensors coated with the P(VDF-TrFE) copolymers blended with Ag-, Au-, and Y-decorated TiO₂-NFs

was enhanced to 1.53 for the red light, 1.54 for the green light, and 1.59 for the blue light, respectively. The enhancement in responsivity and enhancement factor of the IGZO color-tactile sensors can be ascribed to the photon-assisted piezoelectric effect on the P(VDF-TrFE) copolymers blended with metal-decorated TiO₂-NFs, which can be applied in color discrimination for people with deficient color vision via a touch motion.

Figure 5a–d illustrates the schematics of the IGZO color-tactile sensors coated with the P(VDF-TrFE) copolymers blended with metal-decorated TiO₂-NFs at the normal situation, with the illumination of light, with the application of a force, and with the application of a force under the illumination of light, respectively. It is clearly observed that at the normal situation (Figure 5a), the dipoles were randomly distributed within the nanocomposite film, representing the initial current of the IGZO color-tactile sensors. If the light was illuminated on the P(VDF-TrFE)/metal-decorated TiO₂-NFs nanocomposite films, as shown in Figure 5b, the electron–hole pairs were generated within the films; however, there was no influence of the photo-generated carriers on the drain current. By contrast, in Figure 5c, if a force was applied on the nanocomposite films, the dipoles within the piezoelectric films were aligned neatly to induce more electrons within the IGZO channel, contributing to the enhanced current response as revealed in Figure 4a–c. For the samples with the application of a stimulated force under the illumination of light simultaneously (Figure 5d), owing to the nature of piezoelectric films, the dipoles were arranged in order within the P(VDF-TrFE)/metal-decorated TiO₂-NFs nanocomposite films and a built-in electric field of the dipole moments changed the distribution of photo-generated electron–hole pairs. Hence, the electrons would inject into the IGZO channel under the positive V_{BG} , as confirmed by the measurement without the back-gate bias in Figure S13, Supporting Information, resulting in a further increase in drain current of the IGZO color-tactile sensors compared with that of the devices with only the application of a stimulated force in Figure 5c, which is called the photon-assisted piezoelectric effect. The repeatability and response/recovery time of the enhanced piezoelectric response of the IGZO color-tactile sensors coated with the P(VDF-TrFE) films blended with metal-decorated TiO₂-NFs were measured and are shown in Figures S14 and S15, Supporting Information, respectively, exhibiting a remarkable reliability performance of a pressure sensor. Additionally, the response/recovery rates of the sensors were calculated and are summarized in Table S1, Supporting Information, to show an extremely high responsivity to a particular color of light. Therefore, the photon-assisted piezoelectric effect of the IGZO color-tactile sensors is suitable for applications in color discrimination, which will be discussed in Section 2.5.

2.4. Modeling of Photon-Assisted Piezoelectric Behaviors of IGZO Color-Tactile Sensors

To further confirm the current response of the IGZO color-tactile sensors contributed by the piezoelectric and photonic effects, the current equation of traditional transistors was modified to model these bimodal behaviors. Li et al. proposed an equation to simulate the drain current of a thin-film

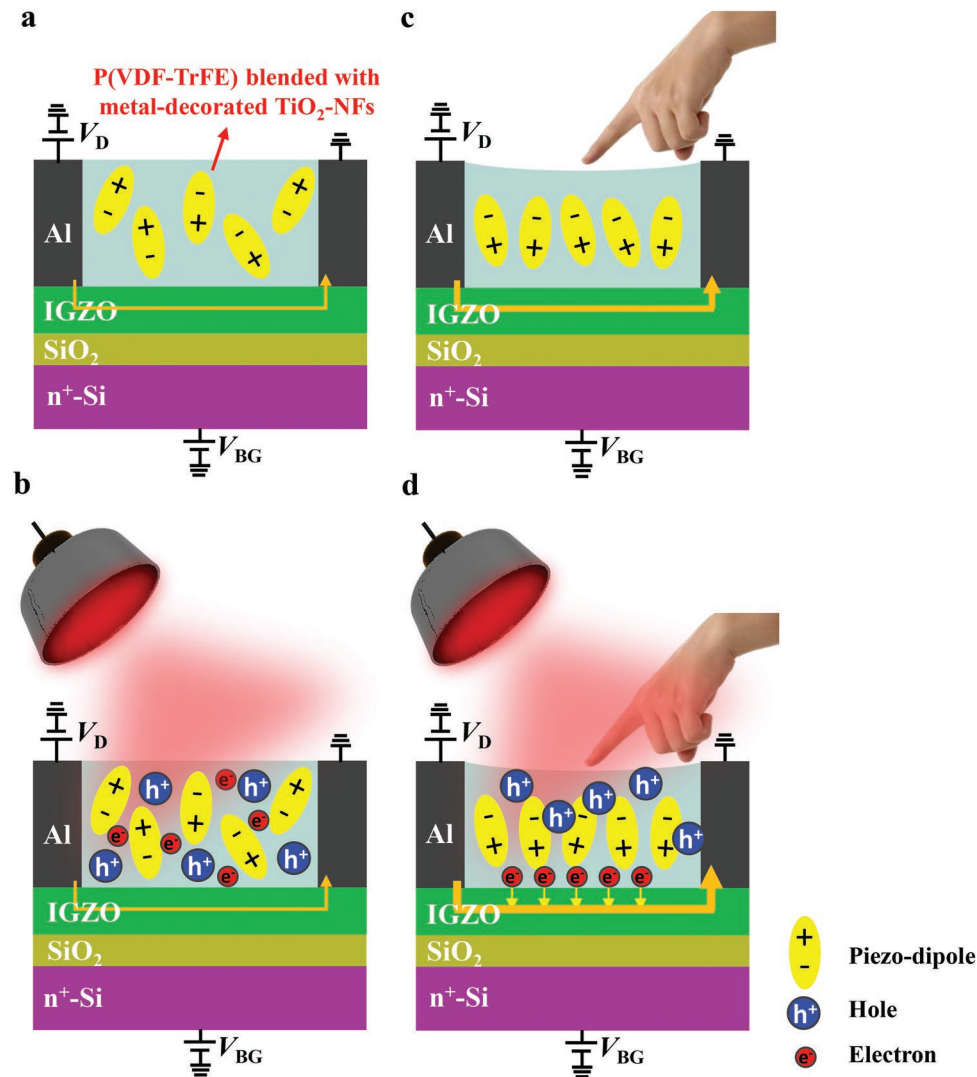


Figure 5. Schematics of the IGZO color-tactile sensors coated with the P(VDF-TrFE) copolymers blended with metal-decorated TiO₂-NFs a) at the normal situation, b) with the illumination of light, c) with the application of a force, and d) with the application of a force under the illumination of light.

transistor (TFT) with piezoelectric charges at the gate for tactile sensing,^[49] which can be used to fit the piezoelectric response of our devices and is expressed as follows:

$$I_{\text{piezo}} = \frac{1}{2} \mu_n C \frac{W}{L} \left[V_{\text{BG}} - \left(V_{\text{T0}} + a \frac{d_{33} F}{C} \right) \right]^2 \quad (4)$$

where C is the capacitance of the back-gate insulator, μ_n is the electron mobility of the IGZO color-tactile sensors, W and L are the channel width and channel length of the devices, respectively, V_{BG} is the back-gate bias, V_{T0} is the threshold voltage of the IGZO color-tactile sensors without any force applied, F is the force applied on the nanocomposite films, d_{33} is the piezoelectric coefficient, and a is a fitting parameter related to the modifications of the P(VDF-TrFE)/metal-decorated TiO₂-NFs nanocomposite films. To simulate the phototronic response, Tai et al. used a current equation of TFTs with a combination

of dark current and unit-lux-current (ULC),^[50] which can be described as follows:

$$I_{\text{photon}} = I_{\text{dark}} + I_{\text{illumination}} = I_{\text{dark}} + (ULC) \times l \quad (5)$$

where I_{dark} is the drain current in the dark, $I_{\text{illumination}}$ is the current generated by the external light, ULC is a parameter related to the illuminance, and l is the illuminance of the light. Additionally, ULC is composed of two portions of the current response, where ULC_1 indicates the drain current at $V_{\text{BG}} < V_{\text{T0}}$ and ULC_2 represents the drain current at $V_{\text{BG}} > V_{\text{T0}}$. Hence, the complete expression of the photon-induced piezoelectric current response can be expressed as follows:

$$I_{\text{photon-piezo}} = \frac{1}{2} \mu_n C \frac{W}{L} \left[V_{\text{BG}} - \left(V_{\text{T0}} + a \frac{d_{33} F}{C} \right) \right]^2 + (ULC_1 + ULC_2) \times l \quad (6)$$

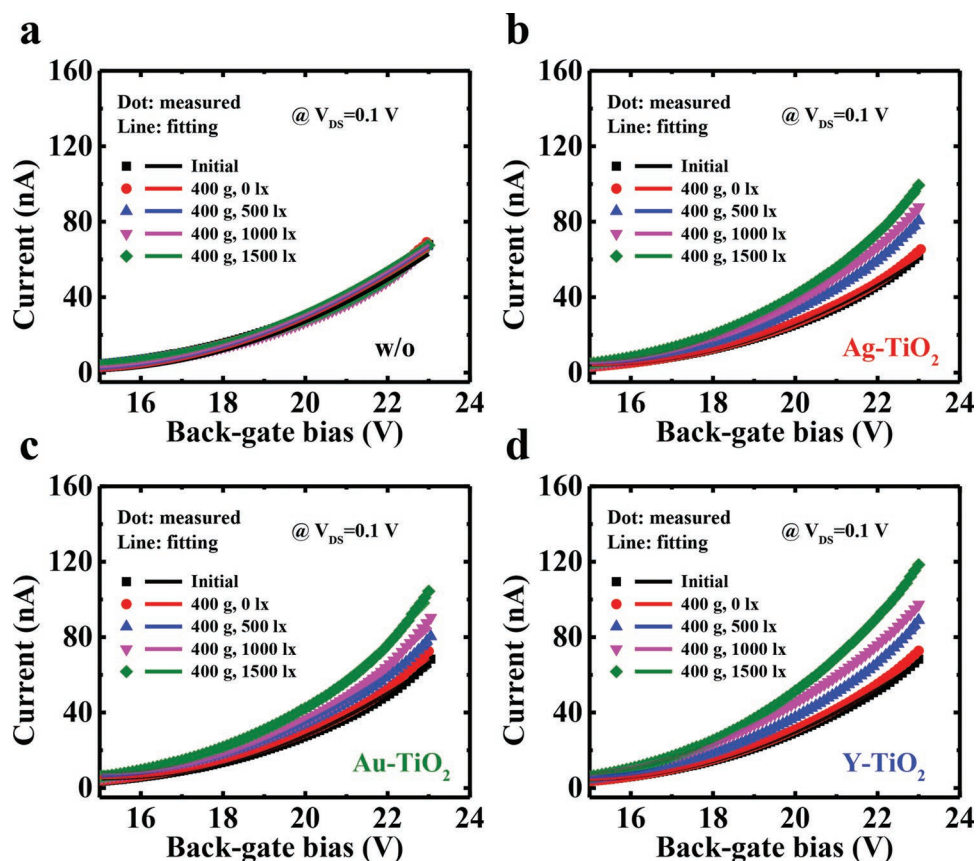


Figure 6. Experimental data and fitting curves of the I_{DS} - V_{BG} transfer characteristics of the IGZO color-tactile sensors coated with a) the pure P(VDF-TrFE) film and the films blended with b) Ag-, c) Au-, and d) Y-decorated TiO_2 -NFs measured at $V_{DS} = 0.1$ V with V_{BG} swept from 15 to 25 V under different illuminances of light at a stimulated force of 400 g.

To carry out the fitting accurately, we focused on the experimental data measured in the range of $V_{BG} > V_{T0}$, that is, ULC_2 . Furthermore, ULC_2 is exponentially related to drain and back-gate biases:

$$ULC_2 = \gamma \exp(\eta_1 V_{DS} - \eta_2 V_{BG}) \quad (7)$$

where η_1 , η_2 , and γ are fitting parameters, representing the exponential dependence on the drain and back-gate biases, and the scaling factor, respectively.

Figure 6 shows the experimental data and fitting curves of the I_{DS} - V_{BG} transfer characteristics of the IGZO color-tactile sensors measured at $V_{DS} = 0.1$ V with V_{BG} swept from 15 to 25 V. The results indicate that the current response can be attributed to the application of a stimulated force and the illumination of external light on the IGZO color-tactile sensors coated with the P(VDF-TrFE) copolymers blended with metal-decorated TiO_2 -NFs. The parameters related to the photon-assisted piezoelectric effects can be extracted from Equations (6) and (7) including η_1 , η_2 , and γ , where η_1 and η_2 are 74.0 and -5.33×10^{-2} , respectively, for all samples. Furthermore, the fitted γ values in the IGZO color-tactile sensors can be obtained as 4.5×10^{-13} , 5.5×10^{-13} , and 7.1×10^{-13} for the P(VDF-TrFE) copolymers blended with Ag-, Au-, and Y-decorated TiO_2 -NFs, respectively. When the wavelength of the external light decreases, for example, the

blue light of ≈ 400 nm, the photon energy excited by the Y-decorated TiO_2 -NFs is higher, resulting in an increase in the fitted γ value for a higher current response of the piezoelectric IGZO color-tactile sensors, as revealed in **Figure 6d**.

2.5. Applications of Photon-Assisted Piezoelectric IGZO Color-Tactile Sensors in Color Discrimination

To investigate the performance of the photon-assisted piezoelectric effect on the P(VDF-TrFE) copolymers blended with metal-decorated TiO_2 -NFs, an LED panel with the alphabets of C, G, and U in three primary colors was fabricated, as shown in **Figure 7a**. The alphabets of C, G, and U in this panel were composed of 6×8 LEDs in red, green, and blue, respectively, as the light source of illumination in the three primary colors for the following measurement. The IGZO color-tactile sensors coated with the P(VDF-TrFE) films blended with Ag-, Au-, and Y-decorated TiO_2 -NFs, respectively, were attached to a human finger through a finger cot for color discrimination of the LED panel, as shown in **Figure 7b**, where the real image of the devices attached to a finger cot is displayed in **Figure 7c**. **Figure 7d** illustrates the equivalent circuit of the sensor array to identify the three primary colors of light with a simple array architecture. A real image of the finger cot with a sensor array

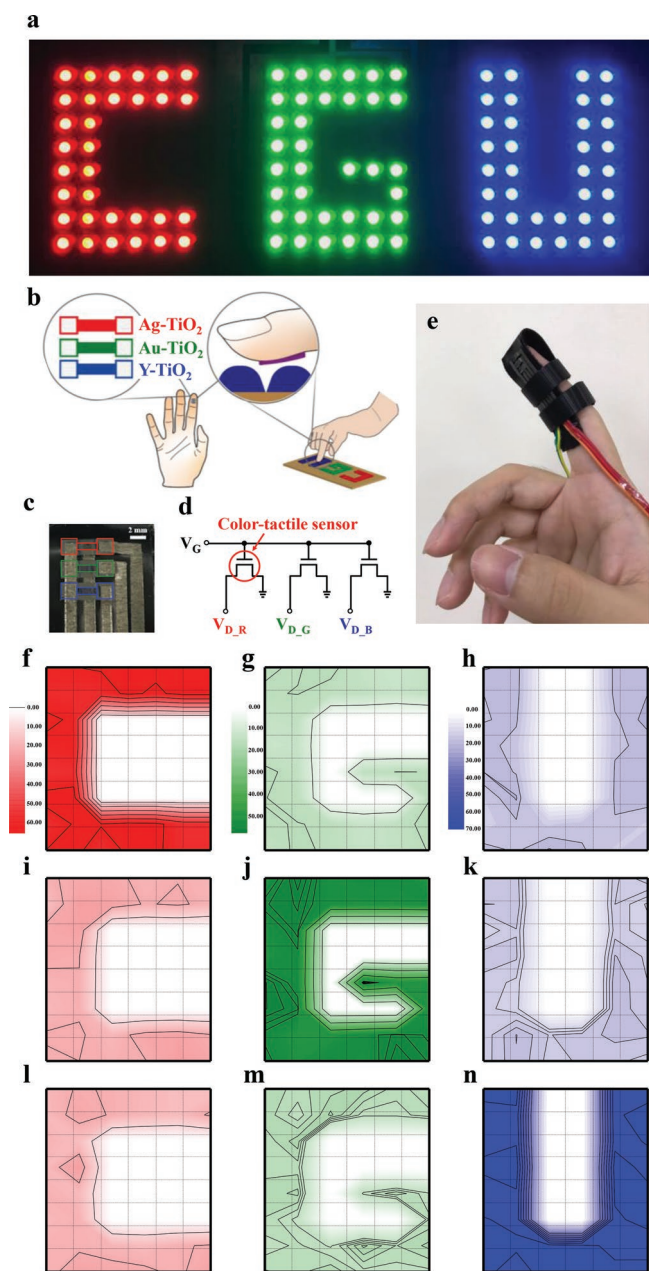


Figure 7. a) An LED panel with the alphabets of C, G, and U in three primary colors. The alphabets of C, G, and U in this panel were composed of 6×8 LEDs in red, green, and blue, respectively, as the light source of illuminations in three primary colors for the following measurement; b) schematics of the IGZO color-tactile sensors coated with the P(VDF-TrFE) films blended with metal-decorated TiO_2 -NFs and attached to a human finger through a finger cot for the color discrimination of the LED panel; c) the real-image of the devices attached on a finger cot; d) the equivalent circuit of the sensor array to identify the three primary colors of light with a simple array architecture; e) the real-image of the finger cot with a sensor array on a human finger; the distributions of the current response of a finger with the sensors coated with the P(VDF-TrFE) films blended with f–h) Ag-, i–k) Au-, and l–n) Y-decorated TiO_2 -NFs to sequentially touch each LED of the panel.

on a human finger is shown in Figure 7e. Then, a finger with the IGZO color-tactile sensors touched the LEDs of the panel

sequentially to obtain the distributions of the current response of each device on the LED panel (Figure 7f–n). When the finger touched the LED panel, the drain current of the IGZO color-tactile sensors coated with the P(VDF-TrFE) copolymers blended with Ag-decorated TiO_2 -NFs appeared to be more sensitive to the panel with the LEDs in red color, that is, the alphabet of C, for an enhancement of $\approx 60\%$ in the current response. On the other hand, for the devices coated with the P(VDF-TrFE) films blended with Au- and Y-decorated TiO_2 -NFs, the current response was significantly enhanced for the panel with the LEDs in green and blue colors, that is, the alphabets of G and U, for the enhancement of 55% and 70% in the current response, respectively. The remarkable result manifests that the IGZO color-tactile sensors coated with the P(VDF-TrFE) copolymers blended with metal-decorated TiO_2 -NFs can recognize the three primary colors of light, suitable for further applications in helping people with deficient color vision to identify different colors of light.

As a practical application for people with deficient color vision, it is necessary to quantify the measurement results using a readable electronic apparatus. Figure 8a shows a schematic of a person employing the IGZO color-tactile sensors on his finger to identify a pseudoisochromatic plate on a tablet. To display the measurement results, the signals were translated from the sensors to a wearable electronic device such as a watch, as depicted in the RGB color wheel of Figure 8b. The watch panel presented the output signal of a bar chart, quantifying it as an RGB color code as indicated in the color wheel. The values of R, G, and B ranging from 0 to 255 in the color code are illustrated, representing all colors via the composition of different numerical values in RGB. For example, the three primary colors (red, green, and blue) can be defined as (255, 0, 0), (0, 255, 0), and (0, 0, 255), respectively. Additionally, a pseudoisochromatic plate with a typical view of 74 was used for a person with deficient color vision to identify red-green color blindness, as shown in Figure 8c,d. The blocks with the largest contrast were presented on a tablet for measurement. Figure 8e,g demonstrates the $I_{\text{DS}}-V_{\text{BG}}$ transfer characteristics of the IGZO color-tactile sensors coated with the P(VDF-TrFE) films blended with metal-decorated TiO_2 -NFs through the touching of coral and sea green portions as presented in the pseudoisochromatic plate on a tablet. To clearly observe the differences in the curves, the $I_{\text{DS}}-V_{\text{BG}}$ characteristics were magnified and are shown in the insets of Figure 8e,g. For the color of coral on the pseudoisochromatic plate, the drain current of the sensors coated with the P(VDF-TrFE) copolymers blended with Ag- and Au-decorated TiO_2 -NFs increased significantly. Compared with the dark current, the RGB color code of coral can be calculated and quantified as 255, 120, and 80 (Figure 8f), corresponding to the actual color code in the color chart.^[51,52] Furthermore, for the color of sea green, the RGB color code can be quantified as 42, 160, and 80 by using the IGZO color-tactile sensors, clearly displayed on the wearable electronic device as shown in Figure 8h. The detailed procedures to quantify the RGB color code of some specific color by using the IGZO color-tactile sensors are presented in the Supporting Information. Through the novel photon-assisted piezoelectricity mentioned above, the IGZO color-tactile sensors

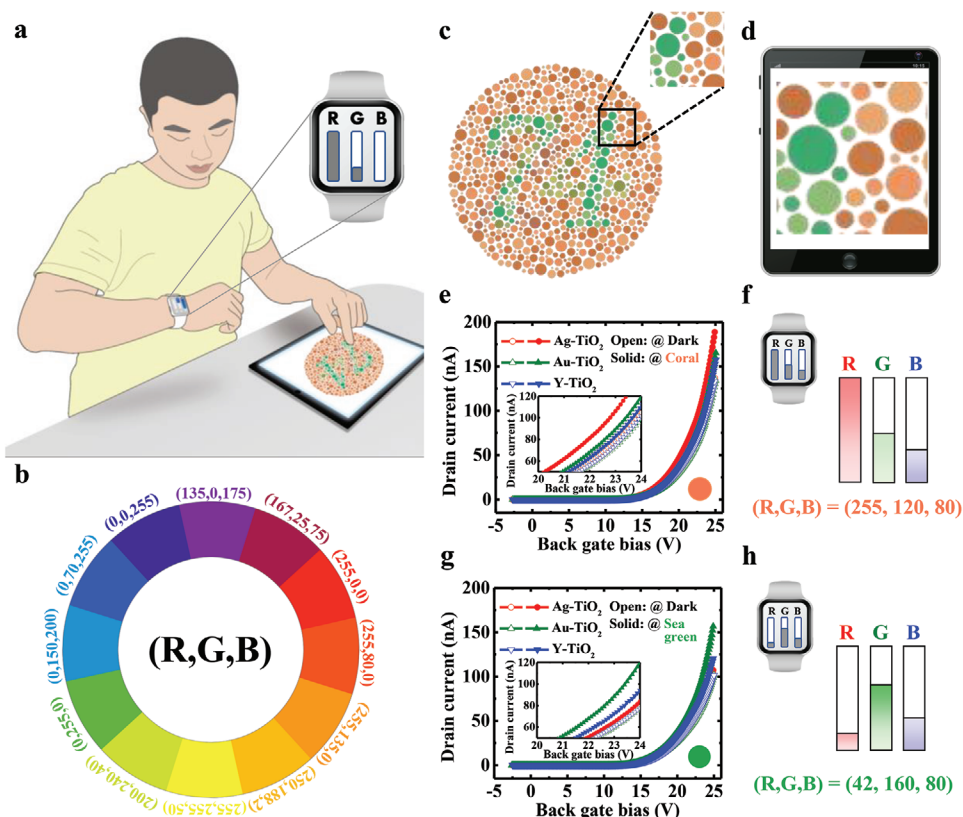


Figure 8. a) A schematic of a person to employ the IGZO color-tactile sensors on his finger for the identification of a pseudoisochromatic plate on a tablet; b) the RGB color wheel to translate the signals from the sensors to a wearable electronic device such as a watch; c,d) a pseudoisochromatic plate with a typical view of 74 presented on a table with the largest contrast to identify the red-green color blindness; the I_{DS} - V_{BG} transfer characteristics of the IGZO color-tactile sensors through the touching of e) coral and g) sea green portions on a tablet of a pseudoisochromatic plate with the magnified scale of the curves shown in the inset figures; the RGB color code of f) coral and h) sea green color displayed on the wearable electronic device calculated from the current response in (e) and (g), respectively, corresponding to the actual color code in the color chart.^[51,52]

coated with the P(VDF-TrFE) copolymers blended with metal-decorated TiO_2 -NFs can be used to identify different colors by a simple touch motion, rendering a promising and new appliance for a person with deficient color vision to regain the ability of color discrimination.

3. Conclusion

In summary, a novel photon-assisted piezoelectric effect realized by IGZO color-tactile sensors with P(VDF-TrFE) copolymers blended with metal-decorated TiO_2 -NFs was proposed. The enhanced crystallinity of the nanocomposite films, the decoration of metal-NPs on TiO_2 -NFs, and the enhanced visible light absorption of each of the metal-decorated TiO_2 -NFs were analyzed via XRD, FTIR, FE-SEM, HRTEM, UV-Vis, and KPFM. With the optimization of blending 5 ppm Ag-, Au-, and Y-decorated TiO_2 -NFs in P(VDF-TrFE) films, the current response of the IGZO color-tactile sensors was significantly enhanced under the application of a stimulated force with the illumination of red, green, and blue colors of light, respectively. The photon-induced electron-hole pairs were generated via LSPR and the electrons were injected into the IGZO channel through the built-in electric field of the dipole moments in the

nanocomposites under the application of a stimulated force, demonstrating the photon-assisted piezoelectric effect with a comprehensive theoretical model. Hence, the IGZO color-tactile sensors were successfully implemented on a finger cot to identify different colors of light on an LED panel with the alphabets and on a tablet with a pseudoisochromatic plate by a simple touch motion. This technology may enable people with deficient color vision to obtain the capability of color discrimination for a more convenient life in the future.

4. Experimental Section

Synthesis of Metal-Decorated TiO_2 -NFs: TiO_2 -NFs were synthesized by a hydrothermal method and further decorated with Ag-, Au-, and Y-NPs. Anatase TiO_2 powder of 25.0 g (Acros Organics, 98+%) was adequately dispersed in a NaOH (Fisher Scientific, >97%) aqueous solution (10.0 M, 62.5 mL) in a Teflon-lined autoclave under vigorous stirring for 30 min. Then, hydrothermal treatment was carried out at 150 °C for 12 h. After treatment, the sodium titanate NFs were washed with deionized water and 0.1 M HCl acid solution (Acros Organics, 37%) until a neutral solution was obtained. Subsequently, a drying process was performed, and the hydrogen titanate NFs were decorated with metal-NPs via wet impregnation. For the metal decoration of 1.0 wt%, 9.5 and 26.1 mg of silver nitrate (AgNO_3 , CHONEYE, extra pure reagent) and yttrium (III) nitrate hexahydrate ($\text{Y}(\text{NO}_3)_3$, Acros Organics, 99.9%), respectively,

were separately dissolved in 200 mL of acetone/ethanol (1:1, v/v). The gold precursor, $\text{H}[\text{AuCl}_4] \cdot 3\text{H}_2\text{O}$ (Acros Organics, $\geq 49.0\%$ Au), was dissolved in H_2O (0.05 g mL^{-1}). Hydrogen titanate NFs (594 mg) were then suspended in these precursor solutions under ultrasonic agitation for 3 h and then stirred for 6 h. After solvent evaporation, a calcination treatment was carried out in a 15% H_2 gas flow with N_2 as a buffer gas for 12 h to obtain TiO_2 -NFs with a final metal decoration of 1.0 wt%.

Fabrication of IGZO Color-Tactile Sensors: IGZO color-tactile sensors coated with P(VDF-TrFE) copolymers blended with metal-decorated TiO_2 -NFs were fabricated. First, the heavily-doped n^+ -silicon wafers ($0.002\text{--}0.005 \Omega\text{cm}$) as the back-gate electrode were cleaned using standard RCA cleaning method to remove contaminants and strip the native oxide on the surface of the Si wafers. Then, a SiO_2 film with a thickness of 50 nm was thermally grown on n^+ -Si wafers via a horizontal furnace at $850 \text{ }^\circ\text{C}$ as the dielectric material. After that, a IGZO film with a thickness of 50 nm was deposited via a DC sputtering system at the power of 100 W using a 3-inch IGZO target (1:1:1:4, 99.99%) as the channel material. The DC sputtering was performed in pure Ar with a gas flow of 20 sccm at a pressure of 6 mTorr. Additionally, the IGZO film was patterned using a shadow mask to define the active region with a channel width of 1 mm. To form the electrodes of the source and drain, an Al film with a thickness of 120 nm was deposited using a thermal evaporator (Al ingot, 99.9999%) at 10^{-6} Torr and defined by a lift-off process. Subsequently, the P(VDF-TrFE) powder (Piezotech, 70:30 mol%) was dissolved in dimethylformamide (Tedia Inc.) to form a 5.0 wt% P(VDF-TrFE) solution. Specific concentrations of Ag-, Au-, and Y-decorated TiO_2 -NFs were mixed into the solution to obtain the P(VDF-TrFE) solutions with 1, 5, and 10 ppm metal-decorated TiO_2 -NFs. Next, the P(VDF-TrFE)/metal-decorated TiO_2 -NFs nanocomposite films were deposited on the IGZO channel by the spin-coating process at a shear stress of 750 rpm for 30 s in a glove box at a pressure of 10 Pa under N_2 to improve the dipole moments of the films. All samples were then baked at $120 \text{ }^\circ\text{C}$ for 4 min to dry the films. To enhance the crystallinity, the P(VDF-TrFE) films/metal-decorated TiO_2 -NFs nanocomposite films were photo-thermally annealed at $120 \text{ }^\circ\text{C}$ for 2 h on a hot plate with an illumination of 1200 lx using white light. After the P(VDF-TrFE)/metal-decorated TiO_2 -NFs nanocomposite films had been formed, the areas of the source and drain were opened for probing via photolithography. Figure S5, Supporting Information, shows the schematic structures of the IGZO color-tactile sensors coated with the P(VDF-TrFE)/metal-decorated TiO_2 -NFs nanocomposite films for the perception of different colors of light via a touch motion.

Material and Device Characterizations: Before the blending of the photocatalysts in the P(VDF-TrFE) films, the visible light absorbance of different metal-decorated TiO_2 -NFs was analyzed using a V-650 UV-Vis spectrophotometer (Jasco International Co., Ltd.). A spherical aberration-corrected field-emission transmission electron microscope (JEM-ARM200FTH, JEOL) was used to observe the microstructure of various metal-decorated TiO_2 -NFs. Additionally, the crystallinity of the P(VDF-TrFE)/metal-decorated TiO_2 -NFs nanocomposites was examined using a Bruker D2 Phaser XRD system through $\text{Cu K}\alpha$ radiation. The angle of incidence, scan steps, and scanning speed for the measurement were $17\text{--}23^\circ$, 0.01° , and $0.0125^\circ/\text{s}$, respectively. To examine the surface morphology of the P(VDF-TrFE)/metal-decorated TiO_2 -NFs nanocomposite films, Hitachi SU8010 FE-SEM with EDS spectra was performed. The film surface was coated with platinum to make the sample conductive and an accelerating voltage of 5 kV was applied. Besides, Bruker Tensor 27 IR with a resolution of 2 cm^{-1} was used to acquire the FTIR spectra and confirm the crystallinity of the nanocomposites. Furthermore, the Dimension-3100 Multimode KPFM (Digital Instruments) was used to measure the contact potential of the films. To investigate the piezoelectric characteristics of IGZO color-tactile sensors coated with P(VDF-TrFE)/metal-decorated TiO_2 -NFs nanocomposite films, a force of 0.1 to 0.4 kg was vertically applied on the device via the JISC MAX-1KN-H automatic load tester equipped with a force gauge through a 2-mm-diameter tip. The electrical behaviors including P - E hysteresis curves and I - E characteristics of the nanocomposite films, and the $I_{\text{DS}}\text{--}V_{\text{BG}}$ transfer characteristics of the IGZO color-tactile sensors, were obtained using a B1500A semiconductor device analyzer (Keysight Technologies).

Supporting Information

Supporting Information is available from the Wiley Online Library or from the author.

Acknowledgements

Y.-P.J. and M.-C.W. contributed equally to this work. The authors would like to thank: 1) Ministry of Science and Technology, R.O.C, Contract Nos. of MOST 109-2221-E-182-032 and MOST 110-2221-E-182-058; and 2) Chang Gung Memorial Hospital, Linkou, Taiwan, Contract Nos. of CMRPD2H0133, CMRPD2J0052, CMRPD2J0053, and BMRPA74 for their financial supports.

Conflict of Interest

The authors declare no conflict of interest.

Data Availability Statement

Research data are not shared.

Keywords

color vision deficiency, color-tactile sensors, photon-assisted piezoelectric effect, poly(vinylidene fluoride-co-trifluoroethylene) (P(VDF-TrFE)), titanium dioxide (TiO_2)

Received: September 2, 2021

Revised: November 9, 2021

Published online: December 24, 2021

- [1] R. Gregory, *Brit. Med. J.* **1998**, *317*, 1693.
- [2] N. Evans, S. Gale, A. Schurger, O. Blanke, *PLoS One* **2015**, *10*, e0130019.
- [3] S. Niketghad, N. Pouratian, *Neurotherapeutics* **2019**, *16*, 134.
- [4] J. C. Blanks, L. V. Johnson, *Invest. Ophthalmol. Visual Sci.* **1984**, *25*, 546.
- [5] C. B. Mellough, E. Sernagor, I. Moreno-Gimeno, D. H. W. Steel, M. Lako, *Stem Cells* **2012**, *30*, 673.
- [6] W. R. Otyola, G. M. Kibanja, A. M. Mugagga, *Makerere J. Higher Educ.* **2017**, *9*, 75.
- [7] J. Voke, *J. Soc. Occup. Med.* **1978**, *28*, 51.
- [8] I. A. M. Suliman, M. S. A. Ali, *Al-basar Int. J. Ophthalmol.* **2017**, *4*, 54.
- [9] C. Caballo, M. Verdugo, *Psychol. Rep.* **2007**, *100*, 1101.
- [10] E. W. Chen, A. S. N. Fu, K. M. Chan, W. W. N. Tsang, *Age Ageing* **2012**, *41*, 254.
- [11] J. H. Shandiz, A. Riazi, A. A. Khorasani, N. Yazdani, M. T. Mostaedi, B. Zohourian, *J. Ophthalmic Vision Res.* **2018**, *13*, 301.
- [12] A. D. Sio, C. Lienau, *Phys. Chem. Chem. Phys.* **2017**, *29*, 18813.
- [13] P. Irkhin, H. Najafov, V. Podzorov, *Sci. Rep.* **2015**, *5*, 15323.
- [14] X. Zhou, F. Yan, S. Wu, B. Shen, H. Zeng, J. Zhai, *Small* **2020**, *16*, 2001573.
- [15] Z. L. Wang, *Nano Today* **2010**, *5*, 540.
- [16] Z. L. Wang, *Adv. Mater.* **2012**, *24*, 4632.
- [17] Z. L. Wang, W. Wu, *Natl. Sci. Rev.* **2014**, *1*, 62.
- [18] Q. Yang, X. Guo, W. Wang, Y. Zhang, S. Xu, D. H. Lien, Z. L. Wang, *ACS Nano* **2010**, *4*, 6285.

- [19] F. Zhang, S. Niu, W. Guo, G. Zhu, Y. Liu, X. Zhang, Z. L. Wang, *ACS Nano* **2013**, *7*, 4537.
- [20] H. Li, Y. Sang, S. Chang, X. Huang, Y. Zhang, R. Yang, H. Jiang, H. Liu, Z. L. Wang, *Nano Lett.* **2015**, *15*, 2372.
- [21] Q. Lai, L. Zhu, Y. Pang, L. Xu, J. Chen, Z. Ren, J. Luo, L. Wang, L. Chen, K. Han, P. Lin, D. Li, S. Lin, B. Chen, C. Pan, Z. L. Wang, *ACS Nano* **2018**, *12*, 10501.
- [22] J. Nie, Y. Zhang, L. Li, J. Wang, *J. Mater. Chem. C* **2020**, *8*, 2709.
- [23] Y. Jiang, L. Gong, X. Hu, Y. Zhao, H. Chen, L. Feng, D. Zhang, *Polymers* **2018**, *10*, 364.
- [24] R. M. Habibur, U. Yaqoob, S. Muhammad, A. S. M. I. Uddin, H. C. Kim, *Mater. Chem. Phys.* **2018**, *215*, 46.
- [25] M. Kim, S. Lee, Y. Kim, *APL Mater.* **2020**, *8*, 071109.
- [26] X. Liu, X. Yang, G. Gao, Z. Yang, H. Liu, Q. Li, Z. Lou, G. Shen, L. Liao, C. Pan, Z. L. Wang, *ACS Nano* **2016**, *10*, 7451.
- [27] M. C. Wu, T. H. Lin, K. H. Hsu, J. F. Hsu, *Appl. Surf. Sci.* **2019**, *484*, 326.
- [28] K. Park, Q. Zhang, D. Myers, G. Cao, *ACS Appl. Mater. Interfaces* **2013**, *5*, 1044.
- [29] M. Madian, A. Eychmüller, L. Giebeler, *Batteries* **2018**, *4*, 7.
- [30] J. Cabrera, H. Alarcón, A. López, R. Candal, D. Acosta, J. Rodriguez, *Water Sci. Technol.* **2014**, *70*, 972.
- [31] N. S. Kumar, S. K. N. Kumar, L. Yesappa, *Mater. Res. Express* **2020**, *7*, 015071.
- [32] L. Kong, X. Zhang, C. Wang, F. Wan, L. Li, *Chin. J. Catal.* **2017**, *38*, 2120.
- [33] Z. Yang, J. Lu, W. Ye, C. Yu, Y. Chang, *Appl. Surf. Sci.* **2017**, *392*, 472.
- [34] J. Singh, K. Sahu, A. Pandey, M. Kumar, T. Ghosh, B. Satpati, T. Som, S. Varma, D. K. Avasthi, S. Mohapatra, *Appl. Surf. Sci.* **2017**, *417*, 347.
- [35] J. Yu, L. Qi, M. Jaroniec, *J. Phys. Chem. C* **2010**, *114*, 13118.
- [36] Y. Soldo-Olivier, A. Abisset, A. Bailly, M. De Santis, S. Garaudée, J. Laciépère, A. Coati, Y. Garreau, M.-C. Saint-Lagera, *Nanoscale Adv.* **2020**, *2*, 2448.
- [37] C. J. Dahlman, A. Agrawal, C. M. Staller, J. Adair, D. J. Milliron, *Chem. Mater.* **2019**, *31*, 502.
- [38] S. Li, P. Miao, Y. Zhang, J. Wu, B. Zhang, Y. Du, X. Han, J. Sun, P. Xu, *Adv. Mater.* **2021**, *33*, 2000086.
- [39] X. Chen, J. Shao, X. Li, H. Tian, *IEEE Trans. Nanotechnol.* **2016**, *15*, 295.
- [40] K. Okimura, J. Sakai, S. Ramanathan, *J. Appl. Phys.* **2010**, *107*, 063503.
- [41] R. I. Haque, R. Vié, M. Germainy, L. Valbin, P. Benaben, X. Boddaert, *Flexible Printed Electron.* **2016**, *1*, 015001.
- [42] M. M. Abolhasania, K. Shirvanimoghaddam, H. Khayyam, S. M. Moosavi, N. Zohdi, M. Naebe, *Polym. Test.* **2018**, *66*, 178.
- [43] T. Feng, D. Xie, Y. Zang, X. Wu, T. Ren, W. Pan, *Integr. Ferroelectr.* **2013**, *141*, 187.
- [44] X. Han, M. Chen, C. Pan, Z. L. Wang, *J. Mater. Chem. C* **2016**, *4*, 11341.
- [45] X. Zhou, S. Wu, C. Li, F. Yan, H. Bai, B. Shen, H. Zeng, J. Zhai, *Nano Energy* **2019**, *66*, 104127.
- [46] N. Yogeswaran, W. T. Navaraj, S. Gupta, F. Liu, V. Vinciguerra, L. Lorenzelli, R. Dahiya, *Appl. Phys. Lett.* **2018**, *113*, 014102.
- [47] J. Sun, P. Li, R. Gao, X. Lu, C. Li, Y. Lang, X. Zhang, J. Bian, *Appl. Surf. Sci.* **2018**, *427*, 613.
- [48] G. Dai, H. Zou, X. Wang, Y. Zhou, P. Wang, Y. Ding, Y. Zhang, J. Yang, Z. L. Wang, *ACS Photonics* **2017**, *4*, 2495.
- [49] W. Li, J. A. Weldon, Y. Huang, K. Wang, *IEEE Electron Device Lett.* **2016**, *37*, 325.
- [50] Y. H. Tai, Y. F. Kuo, Y. H. Lee, *IEEE Trans. Electron Devices* **2009**, *56*, 50.
- [51] N. A. Ibraheem, M. M. Hasan, R. Z. Khan, P. K. Mishra, *ARPN J. Sci. Technol.* **2012**, *2*, 265.
- [52] RapidTables, RGB Color Codes Chart, https://www.rapidtables.com/web/color/RGB_Color.html (accessed: June 2021).